# SIMULATION OF MASSIVELY SEPARATED FLOWS AND ROTATING MACHINE FLOWS USING HYBRID MODELS

F.Miralles[1], B.Sauvage[3], S.Wornom[1], B.Koobus[1], A.Dervieux[2,3], A. Duben[4], V. Bobkov[4], T. Kozubskaya[4]

[1] IMAG, Université de Montpellier, France,
[2] Société LEMMA, Sophia-Antipolis, France
[3] INRIA Sophia-Antipolis, France
[4] CAALAB, Keldysh Institute of Applied Mathematics, Moscow

8th European Congress on Computational Methods in Applied Sciences and Engineering, Oslo, 9 june, 2022

# Overview

**Goal**

This work is motivated by the development of accurate and efficient tools for simulation of acoustic radiation generated by rotating machines


1. Hybrid approach
2. Discussion on airfoil in deep stall
3. Application on rotating frame

- Why massively separated flows and rotating machine ?

Figure – Helicopter blades application, wind turbines and taxi drone

# Modeling of turbulent flow : RANS description

- Compressible Reynolds Averaged Navier-Stokes Equations :

$$\frac{\partial W_h}{\partial t} + \nabla \cdot F_c(W_h) - \nabla \cdot F_d(W_h) = \tau(W_h) \tag{1}$$

# Modeling of turbulent flow : RANS description

- Compressible Reeynolds Averaged Navier-Stokes Equations :

$$\frac{\partial W_h}{\partial t} + \nabla \cdot F_c(W_h) - \nabla \cdot F_d(W_h) = \tau(W_h) \tag{2}$$

- RANS $k - \varepsilon$ Goldberg[1] and $k - R$[2] closure term :

$$\tau^{k-\varepsilon}(W_h) = \left( \overbrace{0}^{\rho}, \overbrace{\mathbf{0}}^{\rho \mathbf{u}}, \overbrace{0}^{\rho E}, \overbrace{\tau : \nabla \mathbf{u} - \rho\epsilon}^{\rho k}, \overbrace{(C_1 \tau : \nabla \mathbf{u} - C_2 \rho\epsilon + E) T^{-1}}^{\rho\epsilon} \right)$$

$$\tau^{k-R}(W_h) = \left( \overbrace{0}^{\rho}, \overbrace{\mathbf{0}}^{\rho \mathbf{u}}, \overbrace{0}^{\rho E}, \overbrace{\mu_t \mathfrak{S}^2 - \rho \frac{k^2}{R}}^{\rho k}, \overbrace{c_1 T_t \mu_t \mathfrak{S}^2 - \min\left(\rho c_2 k, \mu_t \frac{|\Omega|}{a_1}\right)}^{\rho R} \right)$$

1. U. Goldberg, O. Peroomian et S. Chakravarthy. "A wall-distance-free $k - \varepsilon$ model with Enhanced Near-Wall Treatment". In : *Journal of Fluids Engineering* 120 (1998), p. 457-462.
2. Yang Zhang, Md Mizanur Rahman et Gang Chen. "Development of k-R turbulence model for wall-bounded flows". In : *Aerospace Science and Technology* 98 (2020), p. 105681. issn : 1270-9638.

# Modeling of turbulent flow : RANS description

- RANS $k-\varepsilon$ Goldberg and $k-R$ closure term :

$$\tau^{k-\varepsilon}(W_h) = \left( \overbrace{0}^{\rho}, \overbrace{\mathbf{0}}^{\rho\mathbf{u}}, \overbrace{0}^{\rho E}, \overbrace{\tau : \nabla\mathbf{u} - \rho\epsilon}^{\rho k}, \overbrace{(C_1\tau : \nabla\mathbf{u} - C_2\rho\epsilon + E)T^{-1}}^{\rho\epsilon} \right)$$

$$\tau^{k-R}(W_h) = \left( \overbrace{0}^{\rho}, \overbrace{\mathbf{0}}^{\rho\mathbf{u}}, \overbrace{0}^{\rho E}, \overbrace{\mu_t\mathfrak{S}^2 - \rho\frac{k^2}{R}}^{\rho k}, \overbrace{c_1 T_t\mu_t\mathfrak{S}^2 - \min\left(\rho c_2 k, \mu_t\frac{|\Omega|}{a_1}\right)}^{\rho R} \right)$$

- DDES [3] closure term $\rho\epsilon$ or $\rho\frac{k^2}{R}$ is replaced by $\rho\frac{k^{3/2}}{\mathfrak{l}_{ddes}}$ where :

$$\mathfrak{l}_{ddes} = \frac{k^{\frac{3}{2}}}{\epsilon} - f_{ddes}\max\left(0, \frac{k^{\frac{3}{2}}}{\epsilon} - 0.65\Delta\right), \quad \begin{array}{rcl} f_{ddes} & = & 1-\tanh((8r_d)^3), \\ r_d & = & \frac{\nu_t+\nu}{\kappa^2 y^2 \max(\sqrt{\nabla\mathbf{u}:\nabla\mathbf{u}}, 10^{-10})} \end{array}$$

3. P.Spalart et al. "A New Version of Detached-eddy Simulation, Resistant to Ambiguous Grid Densities". In : *Theoretical and Computational Fluid Dynamics* 20 (juil. 2006), p. 181-195.

## Modeling of turbulent flow : RANS description

- RANS Spalart-Allmaras[4] closure term :

$$\tau^{S.A}(W_h) = \left( \overbrace{0}^{\rho}, \overbrace{\mathbf{0}}^{\rho\mathbf{u}}, \overbrace{0}^{\rho E}, \overbrace{\rho c_b|\Omega| - c_{\omega 1} f_\omega \left(\frac{\nu}{d}\right)^2}^{\rho\nu} \right)$$

- DDES closure term $d$ is replaced by $\mathfrak{l}_{ddes}$ where :

$$\mathfrak{l}_{ddes} = \frac{k^{\frac{3}{2}}}{\epsilon} - f_{ddes} \max\left(0, \frac{k^{\frac{3}{2}}}{\epsilon} - 0.65\Delta\right), \quad \begin{array}{rcl} f_{ddes} & = & 1 - \tanh((8r_d)^3), \\ r_d & = & \frac{\nu_t + \nu}{\kappa^2 y^2 \max(\sqrt{\nabla\mathbf{u}:\nabla\mathbf{u}}, 10^{-10})} \end{array}$$

4. P. SPALART et S. ALLMARAS. "A one-equation turbulence model for aerodynamic flows". In : *30th Aerospace Sciences Meeting and Exhibit*.

## Dynamic Variational Multi Scale-LES description

- VMS formulation [5]

$$\left(\frac{\partial W_h}{\partial t}, \chi_i\right) + (\nabla \cdot F_c(W_h), \chi_i) = (\nabla \cdot F_d(W_h), \phi_i) + \left(\tau^{DVMS}(W_h), \phi_i^{'}\right). \quad (3)$$

- VMS closure term with dynamics coefficients $\mathcal{C}_{model} = \mathcal{C}_{model}(\mathbf{x}, t)$ and $Pr_t = Pr_t(\mathbf{x}, t)$

$$\left(\tau^{DVMS}(W_h), \phi_i^{'}\right) = \left(0, \mathbf{M}_S(W_h, \phi_h^{'}), M_H(W_h, \phi_h^{'}), 0, 0\right)$$

where :

$$\mathbf{M}_S(W_h, \phi_i') = \sum_{T \in \Omega_h} \int_T \underbrace{\overline{\rho}(C_S \Delta)^2 |S|}_{\mu_{sgs}} P \nabla \phi_i' d\mathbf{x}, \quad P = 2S - \frac{2}{3} Tr(S) Id$$

$$M_H(W_h, \phi_i') = \sum_{T \in \Omega_h} \int_T \frac{C_p}{Pr_t} \underbrace{\overline{\rho}(C_S \Delta)^2 |S|}_{\mu_{sgs}} \nabla T' \cdot \nabla \phi_i' d\mathbf{x}, \quad \Delta = \left(\int_T d\mathbf{x}\right)^{1/3}$$

and $\phi_h^{'} = \phi_h - \overline{\phi_h}$ where $\overline{\phi_h}$ is computed from macro cells.

---

5. Charbel Farhat, Ajaykumar Rajasekharan et Bruno Koobus. "A dynamic variational multiscale method for large eddy simulations on unstructured meshes". In : *Computer Methods in Applied Mechanics and Engineering* 195.13 (2006). A Tribute to Thomas J.R. Hughes on the Occasion of his 60th Birthday, p. 1667-1691. issn : 0045-7825.

■ Why Dynamic VMS ?

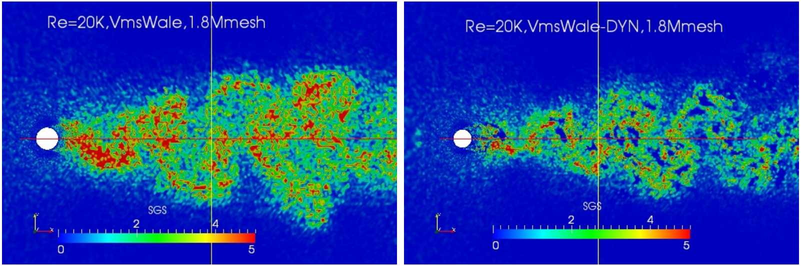


Figure – Flow past a circular cylinder at Re = 20K [6]

6. C.Moussaed et al. "Impact of dynamic subgrid-scale modeling in variational multiscale large-eddy simulation of bluff-body flows". In : *Acta Mechanica* 225 (2014), p. 3309–3323.

- Hybrid description with finite volume/ finite element method

$$\left(\frac{\partial W_h}{\partial t},\chi_i\right)+\left(\nabla\cdot F_c(W_h),\chi_i\right)=\left(\nabla\cdot F_d(W_h),\phi_i\right) \quad (4)$$

$$+\,\theta\left(\tau^C(W_h),\phi_i\right)+(1-\theta)\left(\tau^{DVMS}(W_h'),\phi_i'\right). \quad (5)$$

- ⋆ $\tau^C \in \{\tau^{RANS},\tau^{DDES}\}$
- ⋆ Blending : $\theta = 1 - f_d \times (1-\overline{\theta})$; $\quad \overline{\theta} = \tanh\left(\left(\frac{\Delta}{k^{3/2}}\varepsilon\right)^2\right)$,
- ⋆ $f_d = f_{ddes}$ or $f_d = f_{geo} = \exp\left(-\frac{1}{\epsilon}\min(d-\delta_0,0)^2\right)$

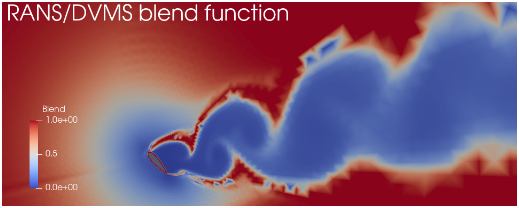


Figure – Hybrid RANS blending surface.

## Set up

- Model used : DDES, RANS/DVMS, DDES/DVMS with :
  - Subgrid model for VMS : Dynamic Smagorinsky
  - Closure model for RANS $k-\varepsilon$ of Goldberg, or $k-R$ or Spalart-Allmaras model.
- Simulation set up :
  - Mach number : 0.1 (subsonic flow)
  - reference pressure : 101300 $[\mathrm{N}/\mathrm{m}^2]$
  - density : 1.225 $[\mathrm{kg}/\mathrm{m}^3]$
  - Wall boundaries conditions :

$$
\begin{aligned}
\mathbf{u}=\mathbf{0}, &\quad \nabla E\cdot\mathbf{n}=0,\ \nabla\rho\cdot\mathbf{n}=0,\\
k-\varepsilon: &\quad k=0,\ \varepsilon=(\nabla\sqrt{k})\cdot\mathbf{n},\\
\text{or } k-R: &\quad k=0,\ R=0,\\
\text{or } S.A: &\quad \nu_t=0.
\end{aligned}
$$

  - The mesh is radial with minimal mesh size is such that $y_w^+ \simeq 0.7 \Leftrightarrow \delta = 5\times 10^{-5}$.

| Name | Mesh size | $y_w^+$ | $\overline{C}_d$ | $\overline{C}_l$ | $St$ |
|---|---|---|---|---|---|
| **Present simulation** | | | | | |
| **DDES SA** Lz = 4c, 201 slices | 6M | 0.7 | **1.49** | **0.91** | **0.20** |
| **DDES SA adapted mesh** Lz = 5c | 0.2M | - | **1.53** | **0.97** | **0.16** |
| **DDES** $k-\varepsilon$ **cubic** Lz = 1c, 33 slices | 0.5M | 0.7 | 1.65 | 1.00 | 0.12 |
| **DDES k-R** Lz = 1c, 33 slices | 0.5M | 0.7 | 1.26 | 1.05 | 0.30 |
| **URANS / DVMS Smagorinsky** Lz = 1c, 33 slices | 0.5M | 0.7 | **1.54** | **0.95** | **0.30** |
| **URANS k-R/ DVMS Smagorinsky fgeo** Lz = 1c, 33 slices | 0.5M | 0.7 | 1.86 | 1.24 | 0.20 |
| **DDES / DVMS Smagorinsky fddes** Lz = 1c, 33 slices | 0.5M | 0.7 | 1.64 | 1.01 | 0.32 |
| **Other simulations** | | | | | |
| **DES/OES** $k-\omega$ Lz=4c [7] | 2M | - | 1.682 | 1.000 | |
| **Experiment** | | | | | |
| Experiments [8] | | | 1.517 | 0.931 | |

Table – Bulk coefficient of the flow around a circular cylinder at Reynolds number 1M, $\overline{C}_d$ holds for the mean drag coefficient, $\overline{C}_l$ is the mean of lift time fluctuation.

7. R. El Akoury et al. "Unsteady Flow Around a NACA0021 Airfoil Beyond Stall at 60 degrees Angle of Attack". In : t. 14. Jan. 2009, p. 405-415. isbn : 978-1-4020-9897-0. doi : 10.1007/978-1-4020-9898-7_35.

8. K. Swalwell. *The effect of turbulence on stall of horizontal axis wind turbines.* 2005.

- Pressure coefficient

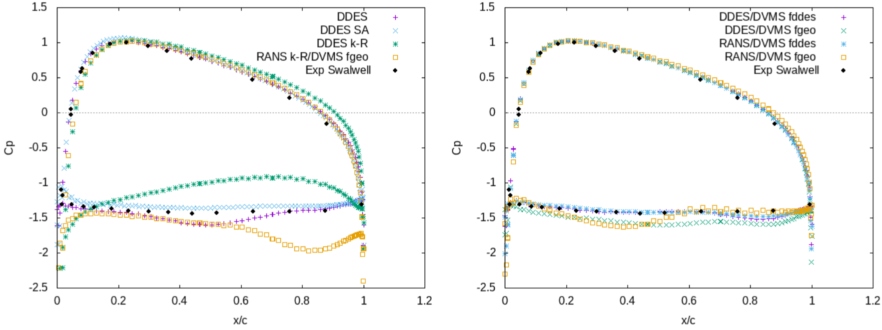


Figure – Distribution of mean pressure as a function of polar angle.

## Vorticity field

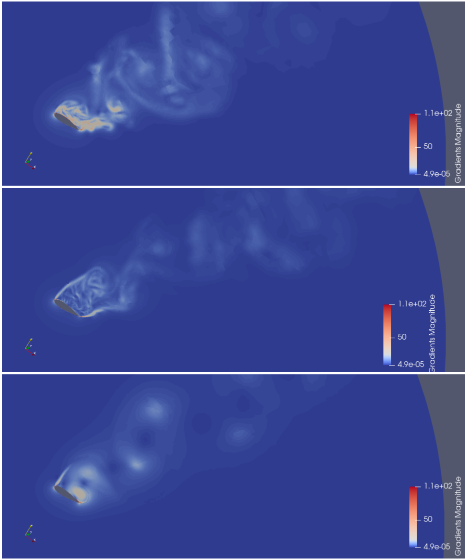


Figure – Vorticity field of DDES on top, hybrid DDES DVMS on middle side and hybrid RANS/DVMS on bottom.

## Model presentation

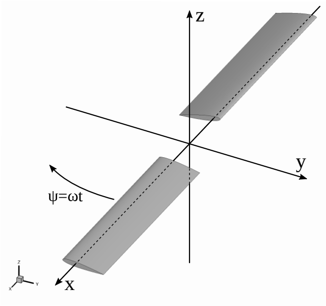


Three computations :

- RANS-SA (3.5M vertices)
- DES (150M vertices)
- RANS-SA adapted mesh (2.2M vertices)

(*)F. X. Caradonna, C. Tung, Technical Report NASA-TM-81232, 1981.

# MRF method and mesh adaptation

- Mesh adaptation

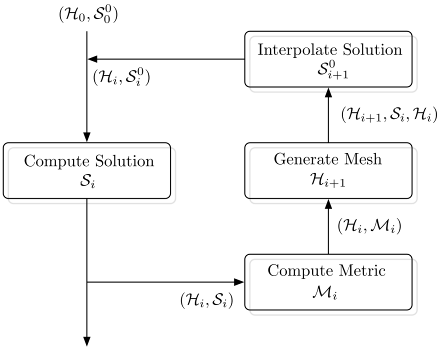


Figure – $\mathcal{H}$, $\mathcal{S}$ and $\mathcal{M}$ are respectively the mesh, the solution and the metric.

- Multiple Reference Frame (MRF)
  - Considering the velocity compositions :

$$\mathrm{u} = \mathrm{u}' + \boldsymbol{\omega} \times \boldsymbol{x}$$

    we rewrite the Navier-Stokes equations in absolute velocity formulation.
  - The computational domain is divided into two sub-domains. A cylindrical box around the helix where $|\boldsymbol{\omega}| = 650$ rpm, and an another cylindrical sub-domain around the box containing the helix where $|\boldsymbol{\omega}| = 0$.

# Numerical results

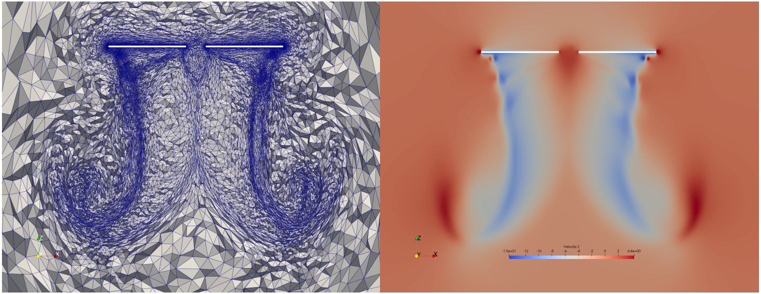


Figure – Caradonna-Tung RANS simulation results : mesh (left) and velocity field (right) in cross-section.

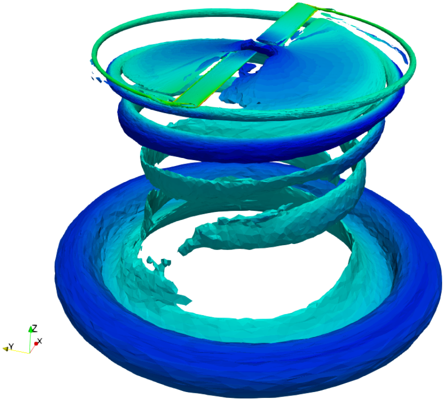

Figure – Caradonna-Tung RANS simulation results : Q-criterion iso-surface.

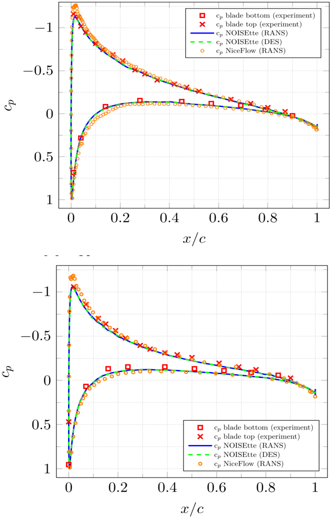


Figure – Pressure coefficient at $r/R = 0.89$ (left) and $r/R = 0.96$ (right) blade sections.

- Conclusion and perspective

  - Bulks coefficients are accurately predicts with RANS/DVMS model and DDES adapted mesh,
  - Hybrid models catch separation of the flow
  - Rotation + DDES on adapted mesh gaves a correct shape of the results

- Use the adapted mesh for RANS/DVMS models.
- Compute aeroacoustic using hybrid modeling.